Postsynthetic high-alumina zeolite crystal engineering in organic free hyper-alkaline media

Article

Post-synthetic high-alumina zeolite crystal engineering in organic-free hyper-alkaline media

Leen Van Tendeloo, Wauter Wangermez, Annelies Vandekerkhove, Tom Willhammar, Sara Bals, Andre Maes, Johan A. Martens, Christine E. A. Kirschhock, and Eric Breynaert

Chem. Mater., **Just Accepted Manuscript** • DOI: 10.1021/acs.chemmater.6b04052 • Publication Date (Web): 20 Dec 2016

Post-synthetic high-alumina zeolite crystal engineering in organic-free hyper-alkaline media

Leen Van Tendeloo[a], Wauter Wangermez[a], Annelies. Vandekerkhove[a], Tom Willhammar[b], Sara Bals[b], André Maes[a], Johan A. Martens[a], Christine E.A. Kirschhock[a], Eric Breynaert[a,*]

[a]Centre for Surface Chemistry and Catalysis, KU Leuven, Celestijnenlaan 200F – box 2461, B-3001 Heverlee, Belgium

[b]EMAT, University of Antwerpen, Groenenborgerlaan 171 - G.U.432, B-2020 Antwerpen Belgium

ABSTRACT: Post-synthetic modification of high-alumina zeolites in hyper-alkaline media can be tailored towards alteration of framework topology, crystal size and morphology, or desired Si/Al ratio. FAU, EMT, MAZ, KFI, HEU and LTA type starting materials were treated with 1.2 M MOH (M= Na, K, Rb or Cs) leading to systematic ordered porosity or fully transformed frameworks with new topology, and adjustable Si/Al ratio. Besides the versatility of this tool for zeolite crystal engineering, these alterations improve understanding of the crystal chemistry. Such knowledge can guide further development in zeolite crystal engineering. Post-synthetic alteration also provides insight in the long term stability of aluminosilicate zeolites that are used as a sorption sink in concrete-based waste disposal facilities in harsh alkaline conditions.

INTRODUCTION

Formation of zeolites, both natural and synthetic, is typically observed when alkaline aqueous fluids interact with aluminosilicates under hydrothermal conditions.[1] Being metastable phases, enthalpies of formation for zeolites with identical compositions such as all-silica zeolite frameworks, are almost identical[2]. Consequently, kinetics and favorable conditions for nucleation and growth are often deterministic for the nature of the zeolite(s) obtained.[3] This explains the successfull application of organic structure directing agents (OSDAs) to assist the crystallization of desired phases and control the outcome of zeolite syntheses. Although detailed mechanisms are only known in exceptional cases,[4-7] OSDA molecules typically exhibit specific interactions with silicate oligomers, impact crystallization kinetics[8] and finally become encapsulated in cages and channels during crystallization. The dominance of kinetics also explains the occurrence of successive phase transformations, whereof many examples are documented. In series of successive phase transformations between zeolites, often an evolution to smaller pores and higher framerwork density and a more negative enthalpy of formation is observed.[8, 9]

Many topologies in the zeolite collection can be synthesized by transformation of other zeolites in hyper-alkaline aqueous media (i.e. > 0.1M [OH^-]). In such conditions, (partial) dissolution can occur as result of framework hydrolysis initiated by reaction of OH^- with the siloxane bond between neighboring T-atoms, which both may be Si, or Si and Al.[10] As hydroxyl anions also act as mineralizing agent catalysing framework bond breaking and formation, their interaction with a zeolite framework can finally result in a zeolite transformation. The outcome of such transformations is highly dependent on the nature and composition of the starting zeolite and on the composition of the reacting solution. This solution may contain silica and/or alumina species, mineralisation agent, alkali and alkaline earth metal cations and OSDA.

Initially, a framework will undergo (in)congruent dissolution, by release of monomers and/or framework fragments. The released alumosilicate-species undergo rapid equilibration. This process continues until the synthesis fluid is saturated in the respective oligomer composition. Subsequently the pool of (alumino-)silicate oligomers in solution is depleted during nucleation and crystallization of a new phase, which in turn may lead to continued dissolution of the first phase, a process called coupled dissolution-precipitation.[11] During such formation and dissolution processes the composition of the liquid and solid phase changes constantly, thereby continuously varying the conditions for nucleation and growth. One example is the synthesis of zeolite omega from an aluminosilicate gel and tetramethylammonium (TMAOH). In this synthesis, the initial formation of phase pure zeolite X depletes Al from the liquid phase.[12] When subsequently the more silicon rich zeolite omega nucleates and incorporates TMA, zeolite X redissolves and serves as Al-source for the omega phase. When a mixture of zeolite X and zeolite omega is exposed to $NaOH_{aq}$, or to a mixed NaOH/TMAOH solution, the zeolite stability order is reversed. Now zeolite omega dissolves to form zeolite X. Addition of extra silicate to adapt the overall Si/Al ratio allows to again stabilize zeolite omega.[12] This is just one example, highlighting the sensitivity of zeolite syntheses and transformations to small, but structure determining changes in the solutions in contact with the zeolite frameworks. It also is noteworthy to mention that

quite often the new phase is first observed on the existing crystals of the dissolving material,[13, 14] which indicates heterogeneous nucleation as a viable pathway, lowering the required supersaturation for the establishment of nuclei. The latter is of advantage as nucleation often is delayed and requires a supersaturation of the liquid in terms of the species leading to the crystalline phase.

Compared to direct syntheses zeolite transformations often present several advantages such as the opportunity to avoid organic templates or replace them with less expensive ones, faster synthesis, etc.[15, 16] In addition, several examples have been reported where post-synthetic alkaline treatment of zeolites allowed to prepare zeolites with an unusual Si/Al ratio, zeolites exhibiting a compositional gradient throughout individual crystals or to synthesize crystals exhibiting a special morphology.[15]

Highly crystalline MFI type zeolite can be obtained without tetrapropylammonium OSDA or seeding by transformation of calcined *BEA zeolite in aqueous NaOH solution ($NaOH_{aq}$) at 150°C.[16] Using FAU as the aluminosilicate source, all MFI syntheses in presence of only $NaOH_{aq}$ failed.[16, 17] Transformation of [Al]-*BEA into [Al]-SSZ-31 (*STO topology) led to an increased aluminium content in comparison to direct syntheses.[18] Recently, CHA zeolite with a Si/Al ratio as high as 8.5 was synthesized starting from FAU zeolite in presence of TEA and NaOH.[19] Addition of OSDA containing seeds to a transformation not only allows to perform the transformation without further addition of OSDA, but also enables the synthesis of core-shell crystals with an Al-rich shell and a Si-rich core. This was shown for the synthesis of LEV crystals, grown from FAU in NaOH in presence of seeds containing choline template.[15, 20]

In addition to zeolite phase transformation, alkaline treatment of zeolite crystals can lead to attractive properties. Post-synthetic generation of pores in high-silica zeolites by controlled alkaline dissolution, called desilication, is very popular.[21] Desilication of zeolite crystals exhibiting a Si/Al gradient or a gradient of defects even allows to generate hollow crystals by coalescence of the intracrystalline voids into a single large cavity.[22] Upon exposure of large ZSM-5 crystals to NaOH solution, typically the interior of the crystals selectively dissolves, while the rim remains intact.[23, 24] The interior likely is more siliceous than the rim explaining its preferential dissolution. This allows to create hollow crystals serving as microcapsules, having a thin shell and large hollow core with potential for applications in many fields.[25] Regular MFI type zeolite microboxes (ca 180 x 350 nm) with a hollow core and intact, thin crystalline shell with uniform thickness were obtained by mild treatment of MFI zeolite crystals with aqueous Na_2CO_3.[26] Upon treatment of calcined Silicalite-1 nanocrystals with TPAOH, Wang *et al*. observed that hollow nanoboxes were formed with zeolitic walls with a thickness of 20-40 nm.[27] It was postulated that Silicalite-1 crystals contain a higher defect probability in the centre of the crystal where growth started. During alkaline treatment the defective crystal core preferentially dissolves. The dissolved silica then recrystallizes on the more stable outer shell, which is further stabilised by adsorbed template. When aluminium is added to the solution, it is incorporated in the zeolite, and ZSM-5 type aluminosilicate nanoboxes are obtained. Occlusion of TPA^+ in the pores further demonstrated that recrystallization indeed took place. Alkaline treatment of Ag containing Silicalite-1 showed that after treatment, Ag particles were no longer protruding from the particles, but were integrated in the shell of the nanocube, again demonstrating recrystallization of silicalite-1 from inside out onto the parent's crystal surface.[28] In the same system, the presence of Na cations led to formation of additional meso- and/or macropores in the shell due to competitive adsorption of Na^+ on the surface, preventing the TPA^+ to play its role as OSDA. Further addition of electrolyte, screening the surface charges of the nanocubes, resulted in the formation of three-dimensional macroporous zeolite monoliths.[28]

Apart from intra-crystal porosity, alkaline treatment also allows to generate and/or widen inter-crystalline pores. Upon treatment with $NaOH_{aq}$ of aggregates of small zeolite crystals (ZSM-5, ZSM-12 and zeolite beta) containing OSDA, inter-crystalline mesopores were formed by congruent dissolution of the outer layers of individual crystallites, thereby preserving the Si/Al ratio as well as the crystallinity.[29] The same process was successfully applied to several commercial mordenites (Si/Al = 5-10) consisting of agglomerated small crystallites. As long as the NaOH solution is sufficiently concentrated, alkaline treatment resulted in an increased porosity due to the formation of inter-crystalline voids. Only for the sample with the highest Si/Al ratio of 10, intra-crystalline mesopores were observed.[30]

Many studies on zeolite crystal engineering dealt with high silica zeolites, which can be modified with mildly alkaline solution. Zeolites with high aluminium content are less soluble and require both stronger alkalinity (hyper alkalinity) and increased temperatures for their modification. This manuscript reports a systematic study of zeolite transformation in hyper alkaline solutions, evaluating the impact of the cation type, liquid to solid ratio, nature of the starting materials, equilibration time and modification of the overall batch composition by addition of Si and/or aluminium in solution. Based on the observed evolution of solid and liquid phases, strategies for crystal engineering of high-alumina zeolites were outlined and experimentally evaluated. The results reported demonstrate how to use post-synthetic hyper alkaline treatment for altering framework topology, crystal morphology, porosity and Si/Al ratio of high-alumina zeolites.

EXPERIMENTAL SECTION

Synthesis of starting materials

Phase pure FAU, KFI, EMT, MAZ, HEU and LTA were synthesized according to the recipes given in Table 1. XRD patterns of all these materials are shown in **Figure SI 1**. Organic templates were removed by calcination for 5 hours at 550°C or 600°C in air using an initial heating rate of 2°C/minute. Following calcination, HEU, MAZ and KFI were ion exchanged with 1 M NaCl solutions (3 times, heated until boiling under reflux for 4h). After this pretreatment, all zeolite powders were rinsed on a Buchner funnel with distilled water until Cl^--free and dried at 60°C.

Table 1: Zeolites used as starting materials for transformation in KOH

Zeolite type	Template	Pre-treatment	Si/Al (ICP)	Ref.
FAU (zeolite Y)	15-crown-5, Na^+	Calcination at 550°C	3.50	[31]
EMT	18-crown-6, Na^+	Calcination at 550°C	4.40	[31]
MAZ	TMA^+, Na^+	Calcination at 600°C, Na exchange	2.80	[32]
HEU	Na^+, K^+	Na-exchange	3.40*	[33]
KFI	K^+, Sr^{2+}, 18-crown-6	Calcination at 550°C, Na exchange	4.28	[32]
LTA	Na^+	/	2.13	[34]

* value determined by ^{29}Si MAS NMR.

Table 2: Modifications of the standard recipe to transform K-Y zeolite into chabazite

Experiment	Zeolite (g)	Conc. KOH	Solution (g)	T, time
Reference	0.3	1.2	10	85°C, 7 days
Addition of 1.61 g TEOS	0.3	1.2	10	85°C, 7 days
Addition of 2 g TEOS	0.3	1.2	10	85°C, 7 days
Increase temp. to 170°C	0.3	1.2	10	170 °C; 2 days
Increase KOH conc. to 7 M	0.3	7	10	85°C, 7 days
Addition of 0.38 g Al(OiPr)3	0.3	1.2	10	85°C, 7 weeks

Impact of different synthesis parameters on alkaline zeolite transformations

Cation type. FAU type zeolite was treated with 1.2 M MOH (M= Na, K, Rb or Cs). The zeolite powder (0.3 g, dried at 60° C) was immersed in the hydroxide solution (18 g) in polypropylene bottles, thus applying a weight based liquid to solid (L/S) ratio of 60, if not stated otherwise. The polypropylene bottles were subsequently incubated at 85°C under end-over-end rotation for 7 minutes up to 16 days.

L/S ratio. The impact of the L/S ratio (9-120) on the transformation of FAU in 1.2M MOH (M= K and Na) at 85°C was investigated.

Starting material. FAU, KFI, EMT, MAZ, HEU and LTA zeolites were contacted with 1.2 M KOH at 85°C using a L/S ratio of 60, under end-over-end rotation, with exposure times of 4 to 60 d, until full transformation was reached Also a clear precursor sol was prepared with the atomic batch composition of the liquid phase measured after 22 h during FAU transformation in 1.2M KOH and L/S ratio of 60, using amorphous sources (precipitated amorphous silica (Hi-Sil233, PQ), aluminum isopropoxide ($Al(OiPr)_3$), KOH and H_2O). This sol was incubated together with the other systems.

Equilibration time. KFI type zeolite, crystallized according to the IZA recipe[32] was exposed to 1.2M KOH at 85°C using a L/S ratio of 60, under end-over-end rotation. The evolution of the crystals was evaluated as function of incubation time using X-ray diffraction and electron microscopy.

Overall batch composition. To exclude any impact of other cations present, FAU, Na-Y (Si/Al = 2.6, Zeocat) was first exchanged in a 1 M KCl solution (3 times). This homoionic K-Y zeolite was incubated statically at 85°C with 1.2M KOH at a L/S ratio of 33 (Table 2) The batch composition for this reference experiment was 13.58 K_2O: 5.6 SiO_2: 1 Al_2O_3: 1093. This reference experiment was also repeated starting from amorphous sources (Hi-Sil233, PQ; $Al(OiPr)_3$). In this case, both the Si and Al sources were dissolved separately, each in part of the KOH solution.Subsequently, the 2 solutions were combined and stirred for 30 minutes. Variations of the zeolite based reference recipe were made by increasing the KOH concentration or adding TEOS or $Al(OiPr)_3$ to the KOH solution. These experiments were initially sampled after 2 hours, and followed up to 6 weeks, until full transformation was reached.

Characterization

At each evaluation time, one sample of the respective series was cooled to room temperature, centrifuged and decanted. The supernatant solution was immediately diluted 50 and 500 times with milliQ water and subsequently analysed with ICP-AES to determine the Si and Al concentration in the supernatant solutions. The evolution of the solids was followed by X-ray diffraction (XRD). High resolution XRD patterns were recorded on a STOE STADI MP diffractometer with focusing Ge(111) monochromator ($CuK\alpha_1$ radiation) in Debye-Scherrer geometry with a linear position sensitive detector (PSD) (6° 2θ window) with a step width of 0.5 degree and internal PSD resolution 0.01 degree. High throughput PXRD screening was performed on a STOE STADI P Combi diffractometer with focusing Ge(111) monochromator ($CuK\alpha_1$ radiation) in transmission geometry with 140°-curved image plate position sensitive detector (IP PSD) from with internal IP PSD resolution of 0.03 degree. Scanning electron microscopy (SEM) was performed using a FEI-Nova Nano-SEM 450. Transmission electron microscopy (TEM) specimens were prepared by suspendinging the crystals in ethanol and applying drops of the suspension on a carbon coated copper grid. The electron tomography results were reconstructed from HAADF-

STEM images using a SIRT reconstruction algorithm. The HAADF-STEM images were acquired using an FEI Tecnai G2 transmission electron microscope operated at an accelerating voltage of 200 kV. The reconstructions of the ANA crystals were based on a tilt series of 37 HAADF-STEM images acquired every 4 degrees, covering a tilt range between -74 - +70 degree. The KFI reconstructions were based on a tilt series of 69 HAADF-STEM images collected every 2 degrees covering a tilt range of -76 - +60 degree. A Bruker AMX300 spectrometer (7.0 T) was used to record ^{29}Si MAS NMR spectra of powder samples packed in 4 mm zirconia rotors spun at a frequency of 6 kHz. The resonance frequency of ^{29}Si at this field is 59.63 MHz. 1000 to 4000 scans were accumulated with a recycle delay of 60 s and a pulse length of 5.0 µs. As chemical shift reference served tetramethylsilane (TMS).

RESULTS

Influence of cation type on zeolite transformation

Transformation of zeolite Y (Si/Al = 2.6) in 1 M alkali metal hydroxide solutions,[35] has demonstrated the phase determining impact of the cation type on the transformations at identical hydroxide concentrations. Studies investigating the transformation of Na-Y zeolite into chabazite in KOH have demonstrated the growth of CHA type crystals on facets of the FAU crystals.[36]

Products. Na-Y zeolite with Si/Al ratio 3.58 was exposed to different alkali metal hydroxide solutions under end-over-end rotation at 85°C using a liquid/solid ratio of 60. In these conditions, ANA and CHA are fully crystallized within 3 days in CsOH and KOH, respectively (**Figure 1,Figure SI 2**). In NaOH, reflections of zeolite P (GIS) were detected by XRD only after 16 days (Figure SI 2). While previously[35] phase pure MER was obtained in RbOH, the FAU zeolite with higher Si/Al ratio used in this work induced the crystallization of both MER and CHA within 8 days. By further increasing the liquid to solid ratio from 60 to 100, almost pure CHA type phase was obtained (**Figure SI 3**).

Evolution of the supernatant solution. During the zeolite transformations, the chemical composition of the liquid phase was analysed. **Figure 2** shows evolution of the Si and Al concentration in the supernatant solution of the transformation systems. For all hydroxide solutions (1.2 M MOH with M= Na, K, Rb or Cs), the dissolved silicon concentration rapidly increased at the start of the transformation experiment to reach a constant value, nearly similar for all hydroxides.(Figure 2) The aluminium concentration initially increased to maximum value, before decreasing again.

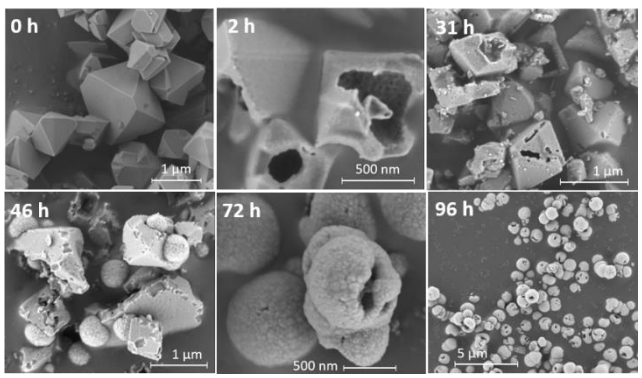

Figure 1: Transformation of zeolite Y in CsOH. After 46 hours the ANA type crystals are clearly recognized.

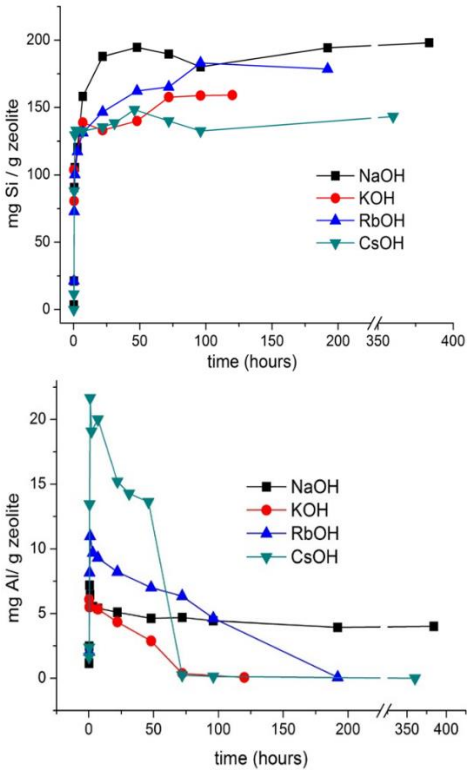

Figure 2: Concentration of dissolved Si and Al during transformation of zeolite Y in 1.2 M MOH.

Upon completion of the conversion, typically a sample dependent concentration is reached. In presence of KOH, CsOH and RbOH, almost all aluminium is reincorporated in the new product. In NaOH however, the dissolved aluminium concentration decreased only slightly after the initial maximum, reaching a constant value in solution instead of being fully incorporated in the growing solid phase. Similar results were obtained using pre-heated alkaline solutions.

Evolution of the solid phase. During transformation of FAU in CsOH, SEM reveals small spherical crystals on the faces of the damaged, hollowed zeolite Y octahedra (Figure 1). In the XRD pattern a small reflection at 26.2° belonging to pollucite, a member of the ANA family, emerges after 46 hours. The formation of the new phase (pollucite) coincides with a steep decrease of the Al content in the solution. Both from XRD and SEM it was observed that the transformation was completed after 72 h. At the same time, also virtually all Al was incorporated in the product. The XRD pattern of the final product indicates broad pollucite reflections which could be related to the very small crystallite size and/or strain in the framework. The spherical pollucite particles, consisting of agglomerated small crystallites (< 100 nm), appear to have a scar, probably originating from their attachment to the zeolite Y crystals during nucleation and initial growth. TEM investigation shows that this scar provides access to an asymmetric void opening up towards one side of the spheres (***Figure SI 4***). The observed morphology of micron sized spheroids consisting of nanocrystalline particles, tens of nm in size, is typical for zeolites with the ANA topology.[37] With the growth of the pollucite crystals, the total weight of the solid phase increased

following an initial decrease as result of the dissolution of the FAU framework (Table SI 1).,

Table 3: Composition of chabazite obtained via transformations with different L/S ratios.

	Q0 Al(%)	Q1 Al(%)	Q2 Al(%)	Q3 Al(%)	Q4 Al(%)	Si/Al
Na-Y (calc)	16.39	54.84	25.70	3.08	0	3.46
CHA, L/S= 9	4.13	26.41	46.74	20.12	2.59	2.10
CHA, L/S = 60	2.77	13.62	32.96	33.96	16.69	1.61
CHA, L/S = 120	2.75	11.35	29.93	34.90	21.08	1.54

During the initial sampling after 22 hours, only hollow FAU crystals were detected. Following separation of solid and liquid phase by centrifugation, continued incubation of both phases separately resulted in the formation of ANA in both the liquid as well as the solid phase. This indicates that ANA forms over a broad range of conditions in presence of CsOH, and that the supernatant solution had a composition favourable for ANA formation. Only when the solid recovered after 22 h was rinsed with water before re-incubation no further transformation occurred. In this case, the NaY proved to be quite stable and did not transform further.

A similar observation was made for the transformation of zeolite Y into ANA in NaOH.[38] It is thus concluded that although no complete phase transformation in NaOH took place within the timeframe studied, the extent of zeolite Y dissolution was similar to the initial situation in the other alkaline solutions. It is clear that hydroxide attack, independent of the alkaline cation, not only removes silicon, but also aluminium from the starting framework. Al is however quickly reincorporated upon crystallisation of a new solid phase.[39]

Influence of L/S ratio on transformation products

In presence of KOH, chabazite is formed from zeolite Y in a broad range of conditions. For L/S ratios from 9 to 120, the transformation always results in chabazite, but the Si/Al ratio of the chabazite product is dependent on the S/L ratio (Table 3), indicating the different liquid volumes extract different relative amounts of Si and Al from the solid phase. Interestingly, the Si/Al ratio of the product is always lower than that of the starting FAU. A chabazite with Si/Al ratio of 2.6 was obtained in a separate experiment starting from a zeolite Y with Si/Al ≈ 6.[35]

In the experiments using KOH and NaOH, for higher L/S ratios, lower concentrations of Si and Al in solution were measured. Still, a higher L/S ratio led to an increased extraction of Si from the solid phase. This is readily reflected in the lower Si/Al ratios observed for CHA transformed using a higher L/S ratio and in the different concentrations of silica dissolved in the supernatant solution upon exposure of NaY to NaOH solutions at different L/S ratios. (**Figure SI 5**) In contrast to the K system where the L/S ratio determines the Si/Al ratio of the final product, in the Na-system the liquid to solid ratio determines the nature of the observed transformation products. Indeed, with L/S ratio of 9, the first reflections appearing are those of ANA, while at L/S = 60, first zeolite P is detected, and only later also reflections of ANA appear (***Figure SI 6***)

Influence of starting materials on products

Zeolite frameworks other than zeolite Y, but with similar framework composition, were exposed to KOH solution. The EMT framework structure, similarly to FAU, was completely transformed into CHA within 4 days at 85°C. However, the HEU and LTA framework structures required 6 to 12 days for transformation, and MAZ even required 30 to 60 days. The XRD patterns of the products obtained after full transformation of the initial materials are shown in **Figure 3**. The long transformation time of the MAZ sample resulted in the formation of crystalline chabazite material with large crystals with smooth surfaces (**Figure 4**). Also the products from FAU, EMT and LTA were identified as pure chabazite.

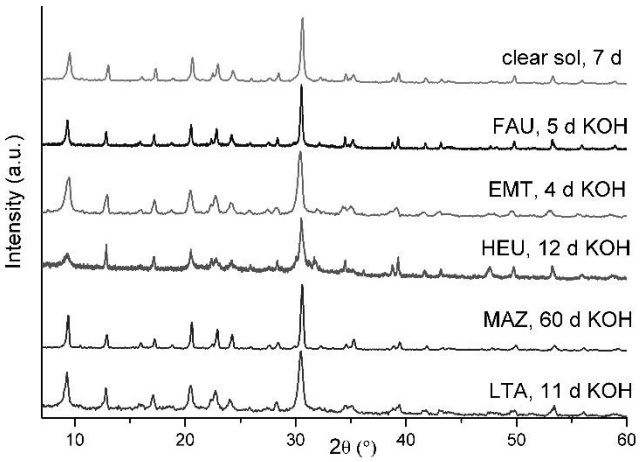

Figure 3: Different chabazite products obtained from different starting materials.

The pattern of the HEU transformation product showed some broadened peaks, and on the SEM pictures rod-shaped crystals were recognized that indicate the presence of an impurity. An LTA type zeolite with Si/Al > 2 is not easily obtained with inorganic cations only,[34] and the LTA (Si/Al = 2.2) starting material synthesized still contained a significant amorphous fraction. Therefore, a high-silica LTA framework was also synthesized according to literature,[32] which contained TMA^+ cations still located in sod cages (Si/Al = 3). These cations cannot be removed without creation of a signification amount of extra-framework aluminium upon calcination. The calcined sample fully transformed into CHA within 14 days. However, when the TMA cations were kept in the framework, the transformation into chabazite occurred very slow, taking 29 days before the first chabazite reflection appeared.

Though all starting zeolites finally transform into CHA upon incubation with KOH, the kinetics of transformation are strongly influenced by the starting framework. EMT and FAU which typically form in Na-systems, quickly

transform. LTA also forms easily in presence of Na^+, but transforms much slower. It should be noted however, that

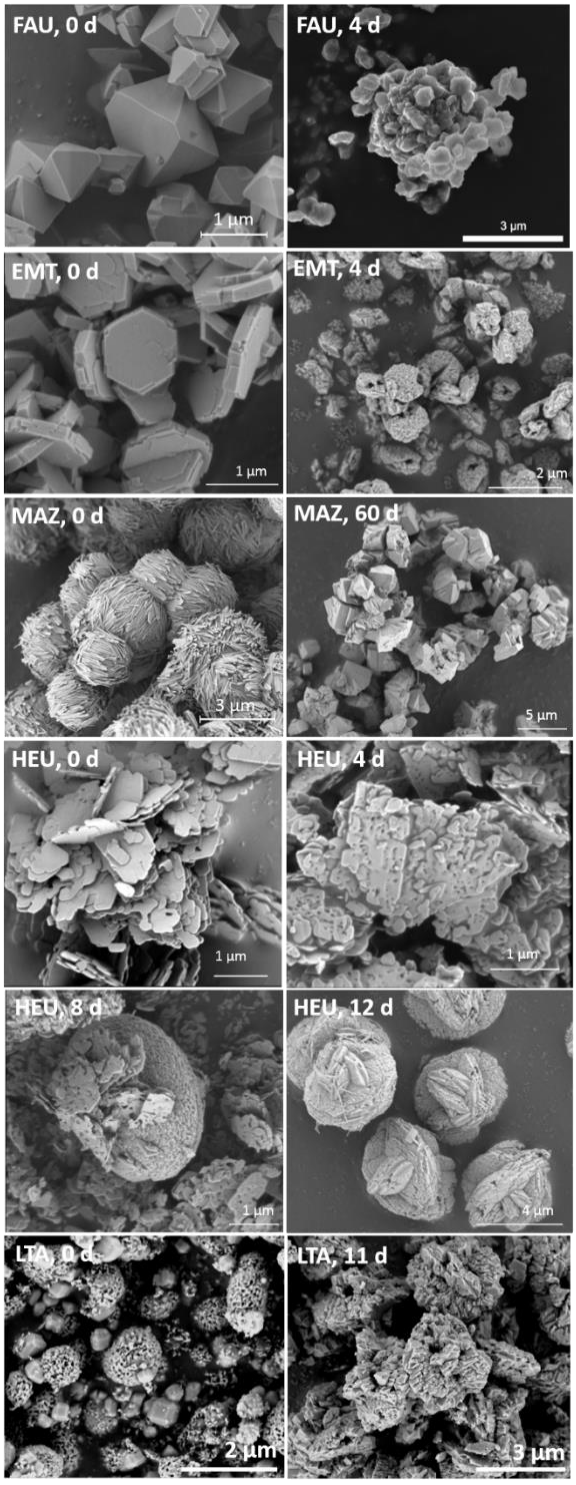

Figure 4: FAU, EMT, MAZ, HEU and LTA type starting materials, and the product formed after full framework transformation in KOH. For HEU, two more intermediate stages are shown.

the LTA sample only had a Si/Al ratio of 2.2, and that such high Al content can stabilize the LTA framework. MAZ,KFI and HEU, which typically crystallise respectively in mixed TMA^+/Na^+, K^+/Sr^{++} or K^+/Na^+, also transform much slower than FAU. These slower transformation kinetics are most likely related to slower dissolution kinetics and/or to a lower solubility of the starting frameworks in KOH. Next to the framework type and density, also other factors determine the transformation kinetics, including the surface area and Si/Al ratio of the starting materials. As the CHA crystals are nucleating on the zeolite source crystals, their final crystal morphology is influenced by it. A related dependence of the final morphology on the kinetic behaviour of the precursor materials has been described by Wilkin for analcime.[40] This type of behaviour results from coupled dissolution and precipitation, a process that has been described for a range of materials much broader than the zeolitefamily.[11]

To investigate the role of the starting framework asides being a steady source for the nutrients leading to CHA and inspired by the formation of pollucite (ANA) in the supernatant solution recovered from the FAU transformation experiment in CsOH (supra), a clear precursor solution was designed to reflect the composition of the liquid phase at onset of CHA formation in the zeolite Na-Y starting material (1.2 M KOH, 2600 ppm Si, 100 ppm Al). From this solution, chabazite crystallized within 7 days and its morphology resembles the chabazite obtained from FAU, MAZ, EMT and LTA (Figure 3,**Figure 5A**). It can be concluded that in this synthesis system the high K^+ concentration compensates most of the impact of the starting framework topology on the final outcome of the transformation. This allows to speculate that equilibration of aluminosilicate oligomers in these K^+ rich, strongly alkaline conditions with a constant L/S ratio leads to similar if not identical oligomer compositions in the supernatant solutions. Consequently, the rate of CHA growth is mainly determined by the rate of dissolution of the starting material.

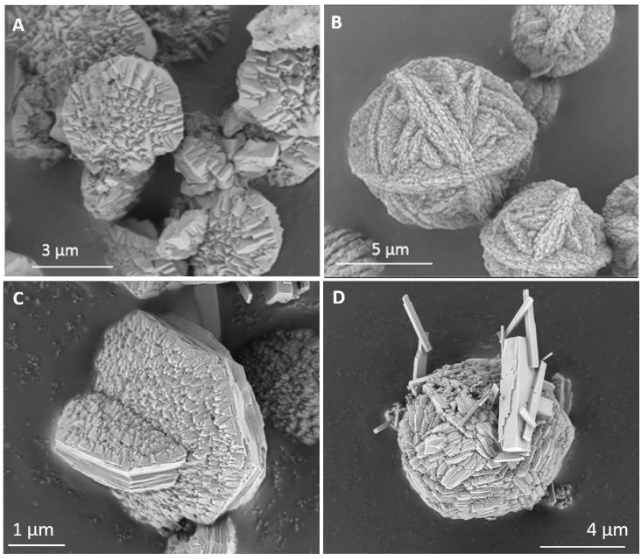

Figure 5: A) Chabazite synthesized from a clear sol with low Al content (7 d) B) Chabazite crystals synthesized from an amorphous obtained (3 weeks) C) and D) The chabazite product obtained when extra aluminium was added to Na-Y and KOH (6 weeks) On image C), the presence of rod-shaped crystals is clearly seen.

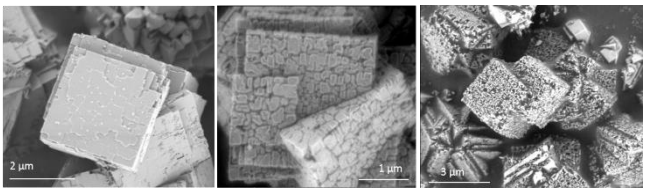

Figure 6: SEM pictures of KFI crystals after 0 days (left), 10 days (middle), and 20 days (right) in KOH.

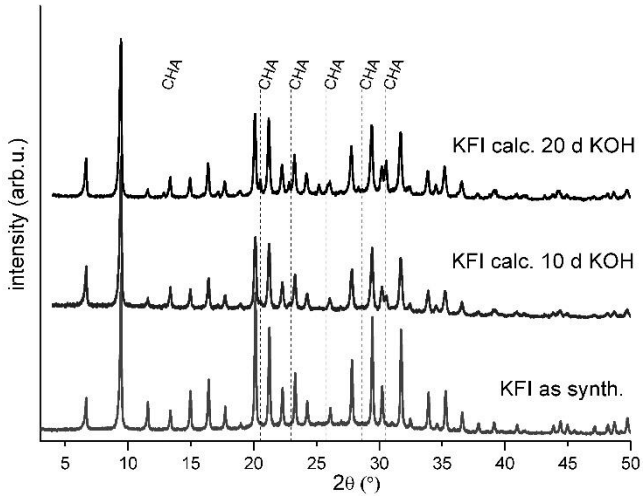

Figure 7: XRD patterns of (wet) as synthesized KFI with 18-crown-6 template. No traces of chabazite are visible in this XRD pattern. After 10 days in KOH, tiny reflections of chabazite have appeared that grow larger in the sample treated for 20 days. Only the CHA reflections that are clearly visible without overlap with KFI are indicated.

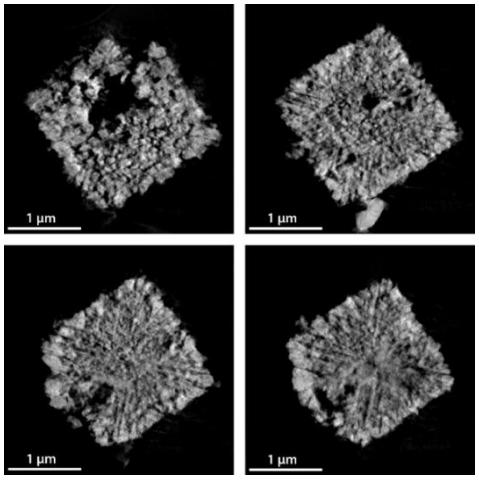

Figure 8: Four orthoslices through the electron tomography reconstuction of a KFI crystal, obtained at different heights, show porosity penetrating the entire crystal.

Influence of equilibration time

By quenching a system before recrystallization has started or has been completed, alkaline treatment of zeolites can be exploited for many more purposes. Transformation of KFI in 1.2M KOH typically results in the formation of CHA. Upon exposure of micrometre sized, intergrown cubes of KFI type zeolite, crystallized according to the IZA recipe[32] to KOH, no transformation takes place within the first 7 days (**Figure 7**). After 10 days in 1.2 M KOH, the crystal surface has changed, and after 20 days the crystals look 'spongy', although the cubic crystal morphology can still be recognized. Only in the last sample, chabazite is clearly recognizable next to these KFI crystals. The chabazite side phase is easily identified from its reflections in the XRD pattern (**Figure 6**) and by electron diffraction (Figure ***SI 7***). On the SEM images, the CHA crystals exhibit a smooth surface and mostly grow on the surface of the KFI crystals (**Figure SI 8**). Though most chabazite crystals are associated with the KFI crystals, also some larger, isolated crystals are found. Morphology and growth of chabazite on the KFI crystals does not seem to be uniform. During the alkaline treatment, the Si/Al ratio of KFI decreases from 4.3 to 2.7 (20 days) (***Table SI 3***).

Similar morphological changes were observed for treatment of ZK-5, synthesized without crown-ether template. However, this starting material already contained traces of chabazite from the start, as this is a common impurity in this KFI synthesis. Investigation of the spongy KFI crystals after 20 days by electron tomography shows porosity penetrating the entire crystals, preferentially running from the edges toward the centre of the crystal.(**Figure 8**) This indicates a preference for the generated pores to terminate with {110} planes. Although most pores have this preferred orientation some are oriented more randomly.

Impact of the overall batch composition.

The main zeolites synthesized in the K_2O-SiO_2-Al_2O_3-H_2O system are EDI, MER, CHA and LTL,[41] next to the less frequently reported ABW, LTJ and BPH[3] types Different synthesis recipes for these frameworks are listed in ***Table SI 2***. From this table, it is concluded that typically, LTL has a higher Si/Al ratio than MER, close to 3, while MER has a Si/Al ratio around 2.[42] It is also seen that for a similar water content, the free alkalinity of LTL syntheses is generally lower, and higher Si/Al ratios are employed. Relative to MER, CHA type zeolite is obtained by lowering the pH by addition of NH_4F,[43] by lowering the synthesis temperature[32] or by decreasing the amount of K^+ cations per SiO_2.[42] EDI has a Si/Al ratio around 1, and is formed at high free alkalinity and low water content.

Starting from standard conditions to transform K-Y into CHA, several parameters were varied which impacted the obtained zeolite framework type (Table 2,Table 3). In the reference experiment, zeolite K-Y was treated with 1.2 M KOH with L/S ratio = 30 at 85°C for 7 days. The total batch composition is given in Table 3 and this synthesis yields CHA with a very small amount of MER impurity after 7 days. At this temperature, CHA is stable in the mother liquor for at least 2 months (***Figure SI 9***). Raising the temperature, increased the MER fraction. Increasing the KOH concentration resulted in EDI formation (**Figure SI 10**).

By addition of silica (either TEOS, precipitated silica or K-silicate solution) to increase the Si/Al ratio of the batch to 10.8, a MER fraction is formed next to CHA (**Figure SI 10**) already at 85°C. When the initial Si/Al ratio is further increased from 10.8 to 12.8, formation of LTL occurs. A transformation of high-silica FAU (Si/Al = 25) to LTL was reported by Honda[17], indicating that LTL seems to form whether or not the silica originates from the dissolving FAU as long the nutrients are available in solution in the correct ratio. Likewise, aluminium rich products can be obtained during transformation by addition of aluminium to

Table 3: Different framework types were obtained by transformation of K-Y in KOH

Experiment	Gel composition	H2O/Si	(KOH-Al)/Si*	FW type
Reference	13.6 K2O: 5.4 SiO2: 1 Al2O3: 1093 H2O	202	4.7	CHA
Addition of 1.61 g TEOS	13.6 K2O : 21.6 SiO2: 1 Al2O3: 1093 H2O	51	1.17	CHA + MER
Addition of 2 g TEOS	13.6 K2O : 25.6 SiO2: 1 Al2O3: 1093 H2O	43	0.98	LTL
Increase temp. to 170°C	13.6 K_2O : 5.4 SiO_2: 1 Al_2O_3: 1093 H_2O	202	4.7	CHA + MER
Increase KOH conc. to 7 M	74 K_2O : 5.4 SiO_2: 1 Al_2O_3: 1093 H_2O	202	27	EDI
Addition of 0.38 g Al(OiPr)3	13.6 K2O: 5.4 SiO2: 3.0 Al2O3: 1093 H2O	202	3.9	CHA

* This parameter is used to express the free alkalinity of the system

the synthesis batch. In this experiment upon treatment of K-Y with Si/Al of 2.7, Al was added to the KOH solution to reach a total batch Si/Al ratio of 1. This reduced the transformation kinetics, and only after 17 days, CHA formation could be detected from the diffraction pattern. After 3 weeks, the XRD pattern hardly changed compared to the pattern at 17 days. After 6 weeks, significant changes occurred though: the FAU framework disappeared and CHA was the major phase present (Figure SI 11). Because the XRD pattern next to sharp peaks, also showed some broad reflections of CHA, it is difficult to designate other phases present.However, the SEM images of this sample, shown in Figure 5, show the presence of rod-shaped crystals. This is the typical morphology of merlinoite, a zeolite with similar formation conditions as CHA, but assignment of MER based on the XRD pattern remained ambiguous.

In this system, with additional Al present, the amount of dissolved Si is low, compared to the standard experiment (***Figure SI 12***). Despite the low Si concentration in solution, the Si/Al ratio of the remaining zeolite Y decreases initially about as much, and after 24 h even more than during the standard experiment (***Table SI 4***). Hence, the decrease in Si/Al ratio of the liquid is mainly attributed to the incorporation of Al in the dissolving FAU framework, which is possible at high pH as evidenced in literature.[44] This finding is also evidenced by the increased weight of the remaining zeolite after 7 weeks: 0.461 g versus 0.3 g of initially added K-Y. The Al incorporation thus has a stabilizing effect on the faujasite and a slower transformation to CHA is the expected result, as evidenced by the transformation into CHA occurring after 6 weeks only. The product has a Si/Al ratio close to 1. Such a low Si/Al ratio of chabazite has only been reported for materials obtained by transformation of metakaolinite in KOH.[45]

Interestingly, when a gel with identical composition as the reference sample was prepared with precipitated amorphous silica and $Al(OiPr)_3$, the 7-day product still was amorphous (***Figure SI 13***). Only after 3 weeks, uniform chabazite crystals were formed. This clearly highlights that kinetics of zeolite formation are not only impacted by the net chemical composition of the synthesis mixture but also by the initial structure of the framework source and especially by its dissolution kinetics which steadily adjusts the compositon of the liquid phase. Indeed, when initially an amorphous gel is formed, the nucleation of CHA takes much longer (3 weeks) as compared to its formation in a clear aluminosilicate sol with low Al content (7 d, supra). The morphology of CHA crystallized from this Al-rich amorphous gel resembles that of the product formed from HEU, while CHA formed from starting phases exhibiting high dissolution and transformation kinetics resemble the phase obtained from a clear precursor sol reflecting the composition of the liquid phase at the onset of CHA formation during transformation of Na-Y.

It thus can be concluded that the main zeolites synthesized in the K_2O-SiO_2-Al_2O_3-H_2O system (EDI, MER, CHA and LTL, supra) are also encountered upon use of zeolite Y as framework source. The parameters inducing the formation of different phases are similar as in the direct syntheses. Although phase pure MER was not obtained in these experiments, it can probably be formed by a combination of higher temperature and higher Si/Al ratio in the batch.

DISCUSSION

The above presented results allow to draw some tentative conclusions, summarized in **Figure 9**. When a zeolite is exposed to an alkaline solution it starts to dissolve, in most cases incongruently. The dissolution rate and silicate species released seem to be determined by the stability of the starting zeolite in the alkaline medium. This means the dissolution kinetics are determined by the original framework structure, its Si/Al ratio and also by the concentration and type of alkali ion of the hydroxide solution. Addition of framework elements like silicate or aluminate to the liquid phase have direct impact, not only on the dissolution rate, but also on the dissolved species as indicated by the lower dissolved silicon concentration and even on the solid phase as shown by the slower transformation kinetics and changing Si/Al ratio with time (Table SI-4). In this case the faujasite withdraws Al from solution, acting as a buffer, adjusting the concentrations of Al and Si in the liquid medium. This example clearly shows the potential to change Si/Al ratios in a zeolite, the final outcome being a material with the same topology but with a modified Si/Al ratio, conveying higher stability to the framework in the used liquid medium.

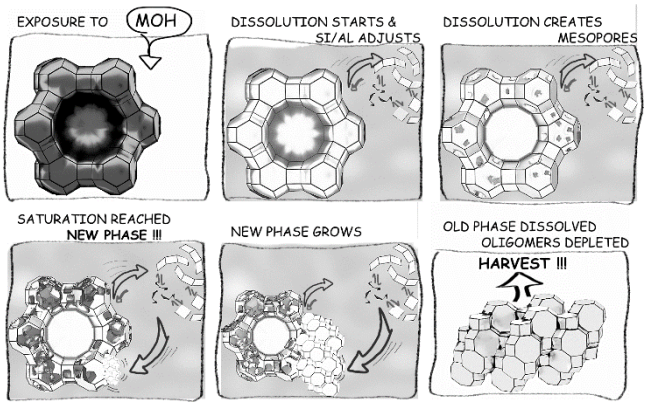

Figure 9: schematic illustration of the effects of hyper-alkaline treatment on alumosilicate zeolites

Dissolution may progress inhomogeneously on mesoscale. Should the framework contain regions with high defect concentration, zoning or structural weakness in certain directions, these parts will dissolve preferentially as concluded from the curious pore structure in the shown case of exposure of KFI to KOH. The aluminosilicate species, either released by the dissolving zeolite or added to the system, rapidly equilibrate in solution. The resulting speciation depends on Si and Al concentration and also type of the alkali cation or other additives. While the resulting composition in the sol has not yet reached saturation level in one or more species the original zeolite keeps dissolving and can be harvested with modified pore structure or with changed Si/Al ratio. For such purposes it is advisable to use a large liquid to solid ratio. In this case, large amounts of the starting framework have to dissolve before the liquid is saturated by aluminosilicate species and formation of a new phase can start.

As soon as supersaturation level of a critical precursor species in the solution is reached, a new zeolite phase can form, assisted by the presence of the original zeolite, which with its already existing tetrahedral network, maybe already contain structural elements of the forming new phase and can serve as nucleation centre. At the same time as the newly growing phase depletes the surrounding liquid of nutrients, the dissolving parent keeps the surrounding liquid at this saturation level and the growth of the new phase proceeds at a rate determined by the dissolution kinetics of the dissolving phase. This can be derived from the observation that the parent framework in most cases persists for a long time next to the newly forming phase. Also the fact that the dissolution kinetics of the parent material depends on the liquid medium and its alumosilicate species adds to this conclusion. In case of rapid depletion of nutrients by the new phase, the original zeolite will dissolve with increased speed, while in the case of slow formation of the new phase also the release of aluminosilicates from the parent is delayed.

The type of newly formed phase obviously exclusively depends on the composition of the liquid phase, as shown from those experiments, where supernatants led to the same framework even after the dissolving parent was removed. Also the observation that addition of aluminate or silicate to the systems allows to change the new zeolite topology from one type to another adds to this. Still, the originally present zeolite framework has decisive impact on the outcome of the synthesis. For one, it offers heterogeneous nucleation centres and therewith significantly shortens long nucleation times. For another, the dissolution kinetics of the starting framework control the concentrations and therewith the speciation of aluminosilicate species in solution and thus also the level of oversaturation. Especially this control avoids formation of a gel-phase, at least on large scale. As shown in the case of chabazite formation from the FAU/KOH/aluminate system, the parent-phase controlled sol leads to the product formation much faster than a gel with the same composition.

All the above conclusions can be used as rough guide how to tune properties of zeolites by hyper-alkaline treatment. However, before a priori prediction of the final outcome of such a treatment becomes realistic, a much more detailed insight in stability, in kinetics and mechanism of zeolite dissolution and in solubility of aluminosilicates in various fluids must be gathered.

CONCLUSIONS

Dissolution and recrystallization in alkaline media provides opportunities for engineering the properties of high-alumina zeolites.

Systematic exploration of the alkaline zeolite transformations confirmed the dominant impact of the alkali metal cation type on the outcome of the transformation. In addition, the liquid to solid ratio, cation concentration and temperature provide handles to direct the transformation to a specific framework. In the K^+ system, temperature and the Si/Al ratio allow to shift between CHA and MER formation. Comparing different starting frameworks with similar Si/Al ratio, the final outcome of the transformation in presence of KOH is always high-alumina CHA. The kinetics of transformation substantially depend on the nature of the starting zeolite. Modifying the L/S ratio in the K^+ system provides a handle to tailor the Si/Al ratio of the final CHA product. In the Na^+ system on the other hand, the liquid to solid ratio determines the nature of the transformation product.

It was shown how alkaline treatment allows to engineer crystal properties such as morphology and Si/Al ratio. By varying the liquid/solid ratio during transformation, by addition of aluminium to the synthesis batch or by post-synthesis alkaline treatment, the product Si/Al ratio can be varied. Precisely timed alkaline treatments allow creation of hollow crystals or single crystals with large intra crystalline pores. Post synthetic modification of high-alumina zeolite by alkaline treatment shows a similar potential as what has already been demonstrated for high-silica zeolites. A better understanding of these transformation process would allow to moree easily combine the optimal zeolitic starting material and treatment conditions to tailor the product properties to a specific application.

ASSOCIATED CONTENT

Supporting Information. XRD patterns and EM images. Overview of syntheses in a K2O-Al2O3-SiO2-H2O system. Synthesis details. Additional information on supernatant solutions, starting materials and products formed. This material is available free of charge via the Internet at http://pubs.acs.org.

AUTHOR INFORMATION

Corresponding Author

*KULeuven, Center for Surface Chemistry and Catalysis. Leuven Chem&Tech, Celestijnen 200F, 3001 Heverlee, Belgium Tel: +3216321598 eric.breynaert@biw.kuleuven.be

Author Contributions

The manuscript was written through contributions of all authors. L.V.T., W.W and A.V. performed the zeolite synthesis and characterization. E.B., A.M., J.A.M., and C.E.A.K. conceived and directed the project. T.W. performed the TEM measurements. All authors have given approval to the final version of the manuscript.

Funding Sources

This work was supported by long-term structural funding by the Flemish Government (Methusalem grant of Prof. J. Martens) and by ONDRAF/NIRAS, the Belgian Agency for Radioactive Waste and Fissile Materials, as part of the program on surface disposal of Belgian Category A waste. The Belgian government is acknowledged for financing the interuniversity poles of attraction (IAP-PAI). G.V.T. and S.B. acknowledge financial support from European Research Council (ERC Advanced Grant no. 24691-COUNTATOMS, ERC Starting Grant no. 335078-COLOURATOMS).

ACKNOWLEDGMENT

L. Van Tendeloo and E. Breynaert acknowledge FWO Vlaanderen as an aspirant and a postdoctoral fellow. This work was partially performed in cooperation with ONDRAF/NIRAS.

ABBREVIATIONS

OSDA, organic structure directing agent; L/S ratio, liquid to solid ratio

REFERENCES

1. Wilkin, R. T.; Barnes, H. L., Solubility and Stability of Zeolites in Aqueous Solution; I, Analcime, Na-, and K-Clinoptilolite. *Am. Mineral.* **1998,** 83, 746-746.
2. Navrotsky, A.; Trofymluk, O.; Levchenko, A. A., Thermochemistry of Microporous and Mesoporous Materials. *Chem. Rev.* **2009,** 109, 3885-3902.
3. Oleksiak, M. D.; Rimer, J. D., Synthesis of Zeolites in the Absence of Organic Structure-Directing Agents: Factors Governing Crystal Selection and Polymorphism. *Rev. Chem. Eng.* **2014,** 30, 1-49.
4. Kirschhock, C. E. A.; Kremer, S. P. B.; Grobet, P. J.; Jacobs, P. A.; Martens, J. A., New Evidence for Precursor Species in the Formation of Mfi Zeolite in the Tetrapropylammonium Hydroxide - Tetraethyl Orthosilicate - Water System. *J. Phys. Chem. B* **2002,** 106, 4897-4900.
5. Verstraelen, T.; Szyja, B. M.; Lesthaeghe, D.; Declerck, R.; Speybroeck, V.; Waroquier, M.; Jansen, A. P. J.; Aerts, A.; Follens, L. R. A.; Martens, J. A.; Kirschhock, C. E. A.; Santen, R. A., Multi-Level Modeling of Silica–Template Interactions During Initial Stages of Zeolite Synthesis. *Top. Catal.* **2009,** 52, 1261-1271.
6. Follens, L. R.; Aerts, A.; Haouas, M.; Caremans, T. P.; Loppinet, B.; Goderis, B.; Vermant, J.; Taulelle, F.; Martens, J. A.; Kirschhock, C. E., Characterization of Nanoparticles in Diluted Clear Solutions for Silicalite-1 Zeolite Synthesis Using Liquid 29si Nmr, Saxs and Dls. *Phys. Chem. Chem. Phys.* **2008,** 10, 5574-5583.
7. Aerts, A.; Follens, L. R. A.; Haouas, M.; Caremans, T. P.; Taulelle, F.; Martens, J. A.; Kirschhock, C. E. A., Combined Nmr, Saxs, and Dls Study of Concentrated Clear Solutions Used in Silicalite-1 Zeolite Synthesis. *Chem. Mater.* **2007,** 19, 3448-3454.
8. Maldonado, M.; Oleksiak, M. D.; Chinta, S.; Rimer, J. D., Controlling Crystal Polymorphism in Organic-Free Synthesis of Na-Zeolites. *J. Am. Chem. Soc.* **2013,** 135, 2641-2652.
9. Chapter I: Synthesis of Zsm-5 Zeolites in the Presence of Tetrapropylammonium Ions. In *Stud. Surf. Sci. Catal.*, Jacobs, P. A.; Martens, J., A. , Eds. Elsevier: 1987; Vol. 33, 47-111.
10. Cundy, C. S.; Cox, P. A., The Hydrothermal Synthesis of Zeolites: Precursors, Intermediates and Reaction Mechanism. *Microporous Mesoporous Mater.* **2005,** 82, 1-78.
11. Ruiz-Agudo, E.; Putnis, C. V.; Putnis, A., Coupled Dissolution and Precipitation at Mineral – Fluid Interfaces. *Chem. Geol.* **2014,** 383, 132-146.
12. Bouchiba, N.; Guzman Castillo, M. L. A.; Benguedach, A.; Fajula, F.; Di Renzo, F., Zeolite Metastability as a Function of the Composition of the Surrounding Solution: The Case of Faujasite and Zeolite Omega. *Microporous Mesoporous Mater.* **2011,** 144, 195-199.
13. Norby, P., Hydrothermal Conversion of Zeolites : An in Situ Synchrotron X-Ray Powder Diffraction Study. *Am. Chem. Soc.* **1997,** 7863, 5215-5221.
14. Wang, Y.; Li, X.; Xue, Z.; Dai, L.; Xie, S.; Li, Q., Preparation of Zeolite Ana Crystal from Zeolite Y by in Situ Solid Phase Iso-Structure Transformation. *J. Phys. Chem. B* **2010,** 114, 5747-5754.
15. Sano, T.; Itakura, M.; Sadakane, M., High Potential of Interzeolite Conversion Method for Zeolite Synthesis. *J. Jpn. Pet. Inst.* **2013,** 56, 183-197.
16. Goel, S.; Zones, S. I.; Iglesia, E., Synthesis of Zeolites Via Interzeolite Transformations without Organic Structure-Directing Agents. *Chem. Mater.* **2015,** 27, 2056-2066.
17. Honda, K.; Itakura, M.; Matsuura, Y.; Onda, A.; Ide, Y.; Sadakane, M.; Sano, T., Role of Structural Similarity between Starting Zeolite and Product Zeolite in the Interzeolite Conversion Process. *J. Nanosci. Nanotechnol.* **2013,** 13, 3020-3026.
18. Ahedi, R. K.; Kubota, Y.; Sugi, Y., Hydrothermal Synthesis of [Al]-Ssz-31 from [Al]-Bea Precursors. *J. Mater. Chem.* **2001,** 11, 2922-2924.
19. Martin, N.; Moliner, M.; Corma, A., High Yield Synthesis of High-Silica Chabazite by Combining the Role

of Zeolite Precursors and Tetraethylammonium. Scr of Nox. *Chem. Commun.* **2015,** 51, 9965-9968.
20. Yashiki, A.; Honda, K.; Fujimoto, A.; Shibata, S.; Ide, Y.; Sadakane, M.; Sano, T., Hydrothermal Conversion of Fau Zeolite into Lev Zeolite in the Presence of Non-Calcined Seed Crystals. *J. Cryst. Growth* **2011,** 325, 96-100.
21. Valtchev, V.; Majano, G.; Mintova, S.; Perez-Ramirez, J., Tailored Crystalline Microporous Materials by Post-Synthesis Modification. *Chem. Soc. Rev.* **2013,** 42, 263-290.
22. Pagis, C.; Morgado Prates, A. R.; Farrusseng, D.; Bats, N.; Tuel, A., Hollow Zeolite Structures: An Overview of Synthesis Methods. *Chem. Mater.* **2016,** 28, 5205-5223.
23. Dessau, R. M.; Valyocsik, E. W.; Goeke, N. H., Aluminum Zoning in Zsm-5 as Revealed by Selective Silica Removal. *Zeolites* **1992,** 12, 776-779.
24. Cizmek, A.; Subotic, B.; Aiello, R.; Crea, F.; Tuoto, C., Dissolution of High-Silica Zeolites in Alkaline Solutions I. Dissolution of Silicalite-1 and Zsm-5 with Different Aluminum Content. *Microporous Mater.* **1995,** 4, 159-168.
25. Li, X.; Zhang, H.; Fang, Y.; Lin, S.; Song, L.; Li, G.; Xin, H.; Li, X., Synthesis and Catalytic Application of Zeolite-Based Hollow Materials. *Energy Environ. Focus* **2014,** 3, 257-265.
26. Mei, C.; Liu, Z.; Wen, P.; Xie, Z.; Hua, W.; Gao, Z., Regular Hzsm-5 Microboxes Prepared Via a Mild Alkaline Treatment. *J. Mater. Chem.* **2008,** 18, 3496-3496.
27. Wang, Y.; Tuel, A., Nanoporous Zeolite Single Crystals: Zsm-5 Nanoboxes with Uniform Intracrystalline Hollow Structures. *Microporous Mesoporous Mater.* **2008,** 113, 286-295.
28. Dai, C.; Zhang, A.; Li, L.; Hou, K.; Ding, F.; Li, J.; Mu, D.; Song, C.; Liu, M.; Guo, X., Synthesis of Hollow Nanocubes and Macroporous Monoliths of Silicalite-1 by Alkaline Treatment. *Chem. Mater.* **2013,** 25, 4197-4205.
29. Van Laak, A. N. C.; Zhang, L.; Parvulescu, A. N.; Bruijnincx, P. C. A.; Weckhuysen, B. M.; De Jong, K. P.; De Jongh, P. E., Alkaline Treatment of Template Containing Zeolites: Introducing Mesoporosity While Preserving Acidity. *Catal. Today* **2011,** 168, 48-56.
30. Van Laak, A. N. C.; Gosselink, R. W.; Sagala, S. L.; Meeldijk, J. D.; De Jongh, P. E.; De Jong, K. P., Alkaline Treatment on Commercially Available Aluminum Rich Mordenite. *Appl. Catal., A* **2010,** 382, 65-72.
31. Feijen, E. J. P.; De Vadder, K.; Bosschaerts, M. H.; Lievens, J. L.; Martens, J. A.; Grobet, P. J.; Jacobs, P. A., Role of 18-Crown-6 and 15-Crown-5 Ethers in the Crystallization of Polytype Faujasite Zeolites. *J. Am. Chem. Soc.* **1994,** 116, 2950-2957.
32. International Zeolite Association, *Verified Syntheses of Zeolitic Materials, 2nd Revised Edition*. 2001; p 177.
33. Satokawa, S.; Itabashi, K., Crystallization of Single Phase (K , Na) -Clinoptilolite. *Microporous Mater.* **1997,** 8, 49-55.
34. Conato, M. T.; Oleksiak, M. D.; Peter Mcgrail, B.; Motkuri, R. K.; Rimer, J. D., Framework Stabilization of Si-Rich Lta Zeolite Prepared in Organic-Free Media. *Chem. Commun.* **2014**, 7-10.
35. Van Tendeloo, L.; Gobechiya, E.; Breynaert, E.; Martens, J. A.; Kirschhock, C. E. A., Alkaline Cations Directing the Transformation of Fau Zeolites into Five Different Framework Types. *Chem. Commun.* **2013,** 49, 11737-11739.
36. Van Tendeloo, L.; Wangermez, W.; Kurttepeli, M.; De Blochouse, B.; Bals, S.; Van Tendeloo, G.; Martens, J. A.; Maes, A.; Kirschhock, C. E. A.; Breynaert, E., Chabazite: A Stable Cation-Exchanger in Hyper Alkaline Concrete Pore Water. *Environ. Sci. Technol.* **2015,** 49, 2358-2365.
37. Kloužková, A.; Mrázová, M.; Kohoutková, M., Synthesis of Partially Stabilized Leucite. *J. Phys. Chem. Solids* **2007,** 68, 1207-1210.
38. Li, P.; Ding, T.; Liu, L.; Xiong, G., Investigation on Phase Transformation Mechanism of Zeolite Nay under Alkaline Hydrothermal Conditions. *Mater. Charact.* **2013,** 86, 221-231.
39. Verboekend, D.; Pérez-Ramírez, J., Desilication Mechanism Revisited: Highly Mesoporous All-Silica Zeolites Enabled through Pore-Directing Agents. *Chemistry* **2011,** 17, 1137-1147.
40. Wilkin, R. T.; Barnes, H. L., Nucleation and Growth Kinetics of Analcime from Precursor Na-Clinoptilolite. *Am. Mineral.* **2000,** 85, 1329-1341.
41. Barrer, R. M., *Hydrothermal Chemistry of Zeolites*. Academic Press: London, 1982; p 360.
42. Skofteland, B. M.; Ellestad, O. H.; Lillerud, K. P., Potassium Merlinoite: Crystallization, Structural and Thermal Properties. *Microporous Mesoporous Mater.* **2001,** 43, 61-71.
43. Liu, B.; Zheng, Y.; Hu, N.; Gui, T.; Li, Y.; Zhang, F.; Zhou, R.; Chen, X.; Kita, H., Synthesis of Low-Silica Cha Zeolite Chabazite in Fluoride Media without Organic Structural Directing Agents and Zeolites. *Microporous Mesoporous Mater.* **2014,** 196, 270-276.
44. Sulikowski, B.; Datka, J.; Gil, B.; Ptaszynski, J.; Klinowski, J., Acidity and Catalytic Properties of Realuminated Zeolite Y. *J. Phys. Chem. B* **1997,** 101, 6929-6932.
45. Thrush, K. A.; Kuznicki, S. M., Characterization of Chabazite and Chabazite-Like Zeolites of Unusual Composition. *J. Chem. Soc., Faraday Trans.* **1991,** 87, 1031-1035.

TOC